Chemistry & Biology, Vol. 12, 1163–1168, November, 2005, ©2005 Elsevier Ltd All rights reserved. DOI 10.1016/j.chembiol.2005.09.013

Investigating β-Hydroxyenduracididine Formation in the Biosynthesis of the Mannopeptimycins

Brad Haltli,[1,*] Ying Tan,[2] Nathan A. Magarvey,[4,5] Melissa Wagenaar,[1] Xihou Yin,[2] Michael Greenstein,[1] John A. Hucul,[1] and T. Mark Zabriskie[2,3,*]
[1]Natural Products Discovery
Wyeth Research
Pearl River, New York 10965
[2]Department of Pharmaceutical Sciences
[3]Program in Molecular and Cellular Biology
Oregon State University
Corvalis, Oregon 97331
[4]Department of Microbiology
[5]Department of Biotechnology
University of Minnesota
Minneapolis-St. Paul, Minnesota 55455

Summary

The mannopeptimycins (MPPs) are potent glycopeptide antibiotics that contain both D and L forms of the unique, arginine-derived amino acid β-hydroxyenduracididine (βhEnd). The product of the *mppO* gene in the MPP biosynthetic cluster resembles several non-heme iron, α-ketoglutarate-dependent oxygenases, such as VioC and clavaminate synthase. The role of MppO in βhEnd biosynthesis was confirmed through inactivation of *mppO*, which yielded a strain that produced dideoxy-MPPs, indicating that *mppO* is essential for generating the β-hydroxy functionality for both βhEnd residues. Characterization in vitro of recombinant His_6-MppO expressed in *E. coli* revealed that MppO selectively hydroxylates the β carbon of free L-enduracididine.

Introduction

The mannopeptimycins (MPPs), produced by *Streptomyces hygroscopicus* NRRL 30439, are a group of cyclic glycopeptide antibiotics with potent activity against methicillin-resistant staphylococci and vancomycin-resistant enterococci (Figure 1) [1]. The MPPs are distinguished by the presence of two stereoisomers of the nonproteinogenic amino acid β-hydroxyenduracididine (e.g., MPP-γ, **1**) [2]. The route of β-hydroxyenduracididine (βhEnd) formation is not known, but the presence of a guanidine moiety suggests that βhEnd is derived from arginine. Arginine is also the precursor to capreomycidine, an amino acid possessing a six-membered cyclic guanidine side chain that is common to the tuberactinomycin antibiotics, including viomycin [3]. VioC is a non-heme iron, α-ketoglutarate-dependent oxygenase that operates in the viomycin pathway and converts free L-Arg to 3*S*-OH-L-Arg [4, 5]. VioD, the product of the gene immediately downstream of *vioC*, then catalyzes the pyridoxal phosphate-dependent conversion of 3*S*-OH-L-Arg to 2*S*,3*R*-capreomycidine [5, 6].

*Correspondence: haltlib@wyeth.com (B.H.); mark.zabriskie@orst.edu (T.M.Z.)

The MPP biosynthetic gene cluster (N.A.M. et al., submitted) contains a gene (*mppO*) with a deduced amino acid sequence that showed end-to-end similarity to VioC (58% similarity, 42% identity) and clavaminate synthase (46% similarity, 31% identity) [7–9]. Clavaminate synthase (CS) is another Fe(II)/α-ketoglutarate-dependent oxygenase that catalyzes nonsequential β-hydroxylation, oxidative cyclization, and dehydrogenation reactions in the conversion of deoxyguanidinoproclavaminic acid to the β-lactamase inhibitor clavulanic acid [9]. Based on the similarity to CS and VioC, we predicted that MppO would catalyze one or more reactions in the conversion of L-Arg to βhEnd. We report here the results of *mppO* inactivation experiments in the producing organism and the in vitro enzymatic characterization of His_6-MppO.

Results and Discussion

Sequence Analysis

The predicted product of *mppO* consists of 341 amino acids and shows significant similarity to CS1 and CS2 [9] and several CS-like proteins, including VioC [7, 8]. In addition to the overall similarity, MppO and its homologs possess a 2-His-1-carboxylate motif common to non-heme iron oxygenases [10]. This motif is generally characterized by the sequence His-Xaa-Asp/Glu_{53-59}-His and is responsible for binding Fe(II). A variant of this model was proposed to describe the key active site residues of CS2 [11]. In the His-3 variant of the 2-His-1-carboxylate model, the second active site histidine residue is separated from the first by 134 aa. In their examination of α-ketoglutarate-dependent, non-heme oxygenases, Khaleeli et al. [11] identified a subset of enzymes that exhibit the His-3 motif, and X-ray crystallography confirmed involvement of the His-1 and His-3 motifs in binding Fe(II) [12–14]. MppO and its homologs (Figure 2) also contain the characteristic His-1 (HXE) and His-3 (DNXXXXH) motifs, and the spacing between these motifs (131–153 aa) is consistent with that observed for CS1 and CS2 (134 aa). Based on these observations, MppO and its homologs likely belong to the His-3 variant group of non-heme iron oxygenases.

Inactivation of *mppO* in *S. hygroscopicus* NRRL 30439

To assess the role of *mppO* in MPP biosynthesis, the gene was inactivated in the producing organism by replacing a 762 bp fragment of the gene with the kanamycin-resistance gene *aphII*. Deletion of the 762 bp fragment removed the entire His-1 motif predicted to be required for Fe(II) binding. The disruption construct (pBWA29) was introduced into *S. hygroscopicus* NRRL 30439 by intergeneric conjugation (N.A.M. et al., submitted). Kanamycin-resistant colonies were selected and screened for double crossover events by Southern blot analysis, and one exconjugant (WPN105) was found in which *mppO* had been replaced with *aphII* (data not shown).

The metabolite profiles of the wild-type and *mppO*$^-$ mutant strains were analyzed by LC/MS. The wild-type culture produced primarily MPP-γ, -δ, and -ε, whereas

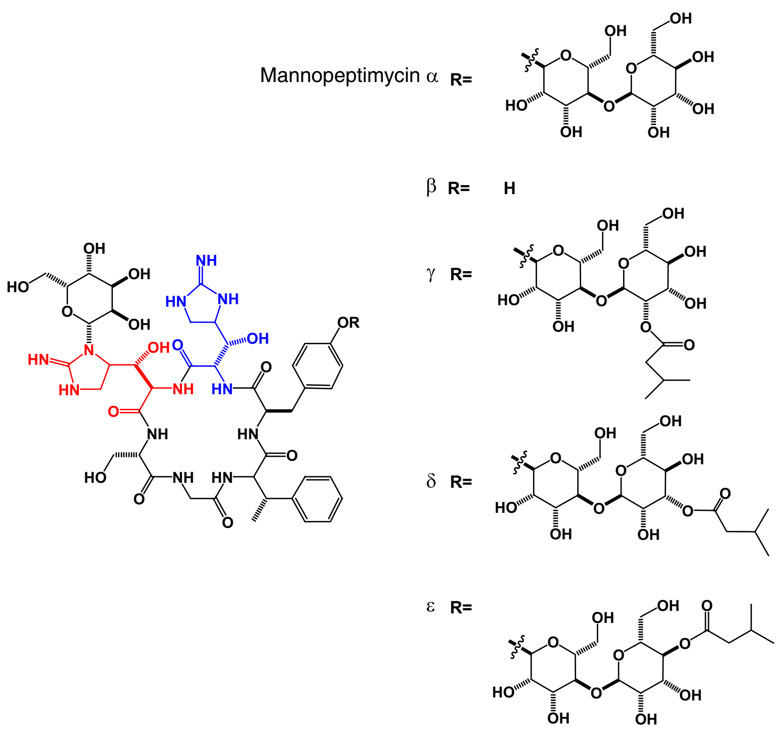

Figure 1. Structure of Natural Mannopeptimycins Produced by *S. hygroscopicus* NRRL 30439

The L-βhEnd residue is blue, and the D-βhEnd residue is red.

the mutant produced a similar array of compounds exhibiting the same UV profile as the MPPs, but having different retention times and masses that corresponded to a loss of two oxygen atoms (HRFTMS-ESI calculated for $C_{59}H_{88}N_{12}O_{24}{}^{2+}$ $[M + 2H]^{2+}$ 674.30117; found 674.30054). Presumably, this finding reflects the absence of two hydroxyl groups. Interestingly, MPP titers from the wild-type and mutant strains were similar, despite evidence from investigation of the MPP adenylation (A) domain substrate specificity that revealed that βhEnd was clearly the preferred substrate and enduracididine (End) was activated at levels similar to negative controls (N.A.M., submitted). A more detailed examination of the βhEnd-incorporating A domain and investigation of possible contributions of the βhEnd-incorporating condensation domains to substrate selectivity is needed.

To determine if the missing hydroxyl groups were from the βhEnd residues or the mannose units, the purified product from the *mppO* mutant fermentation was compared by LC/MS to authentic dideoxy-MPP-γ and -δ. The authentic samples were isolated from an N-methyl-N′-nitro-N-nitroso-guanidine (NTG)-mutagenized strain of *S. hygroscopicus* NRRL 30439 that produces MPPs in which the β carbons of both End residues are not hydroxylated (J. Lotvin, personal communication). Coinjection resulted in an increase in the amount of dideoxy-MPP-γ (Figure 3), confirming that MppO is responsible for introducing the β-hydroxy group of both the D- and L-βhEnd residues.

Sequence Analysis of the NTG-Mutagenized Dideoxy-MPP Producer

To verify if a lesion in *mppO* in the NTG mutant (NRRL 30450) was responsible for the phenotype, *mppO* was amplified from the genomes of the wild-type (NRRL 30439) and mutant strains (NRRL 30450 and NRRL

```
                       A                               B
AsnO   153 aa- FHNENAFHE -105 aa- VTHRLLPGELAIVDNRVTVHGRTEFTPR
SttL   152 aa- WHTEDAFHP -122 aa- REVVADQGDVLFIDNHRAVHGRLPFKAH
VioC   142 aa- WHTEDAFSP -121 aa- YELVLDQGDVAFIDNRRAVHGRRAFQPR
MppO   144 aa- WHTEDAFHP -127 aa- SGVVLSPGDIVFIDNYRVVHGRKPFRAR
CS1    143 aa- FHTEMAYHI -108 aa- VGVKLVPGDVLIIDNFRTTHARTPFSPR
CS2    152 aa- FHTEMAYHI -108 aa- VGVKLVPGDVLIIDNFRTTHARTPFSPR
               :*.* *:                    *:: ::**  ..*.*  * .

                      C
AsnO    -8 aa-  QRTFVLTDLRRSRAMRPADGYVLGAAP
SttL    -8 aa-  KRVCVTADLRRSREMRATAATRLLG--
VioC    -8 aa-  KRINITRDLHRSRKAWAGDSRVLGQR-
MppO    -8 aa-  RRLNIARDLRKSREARLAATTRVIY--
CS1     -8 aa-  HRVY-----------------------
CS2     -8 aa-  HRVYIRTDRNGQLSGGERAGDTISFSP
                :*
```

Figure 2. Sequence Alignment of Key Motifs Found MppO and Related Proteins

ClustalW alignment of (A) His-1, (B) His-3, and (C) His-2 motifs of MppO and its homologs. Results are shown for AsnO from *Streptomyces coelicolor* [17], SttL from *Streptomyces rochei* F20 (direct deposit to the data bank by F. Malpartida, accession number CAB67713), VioC from *Streptomyces vinaceus* [7, 8], MppO from *Streptomyces hygroscopicus* NRRL 30439 [10], and CS1 and CS2 from *Streptomyces clavuligerus* [9]. Invariant residues are indicated with an asterisk. Positions with conservative substitutions are indicated with a colon. Positions with semiconservative substitutions are indicated with a period. Residues proven to be essential for CS2 activity are shaded. The residue proposed by this study to affect activity of MppO is in bold type.

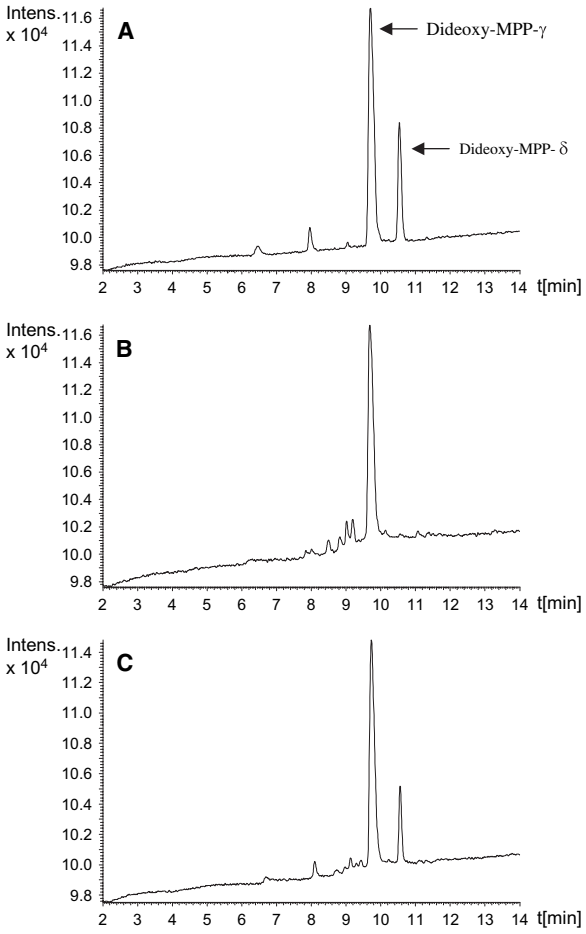

Figure 3. LC/MS Comparison of Putative Dideoxy-MPP-γ Isolated from Mutant WPN105 to Authentic Dideoxy-MPP-γ and -δ Standards

(A) Dideoxy-MPP-γ and -δ standards.

(B) Putative dideoxy-MPP-γ isolated from mutant WPN105.

(C) Coinjection of (A) and (B).

30443). *S. hygroscopicus* NRRL 30443 is the parent strain of NRRL 30450 and produces the normal suite of MPPs. *mppO* was amplified from each strain by PCR and was cloned into pCR-BluntII. Eight clones from each strain were sequenced. There was no difference in the *mppO* sequences from the wild-type strain and NRRL 30443. However, a single point mutation (C→T) at nucleotide 450 was identified in *mppO* from the NRRL 30450 strain. This mutation results in a conservative change wherein an invariant alanine at position 150 is mutated to valine. This mutation does not directly affect residues in the predicted active site (Figure 2), but it is proximal to the essential residues of the His-1 motif (H146 and E148), and the added bulk may hinder the ability to bind Fe(II).

Functional Expression and Characterization of MppO

To complement the gene disruption results and address MppO substrate and stereospecificity issues, *mppO* was amplified by PCR and cloned into pET28a for expression in *E. coli*. This construct was expected to yield a protein with an N-terminal His_6 tag and a calculated molecular weight of 38.6 kDa. After expression, the recombinant protein was purified by metal affinity chromatography, and the efficiency of purification was verified by SDS-PAGE (Figure 4A).

Purified His_6-MppO assays included 1 mM α-ketoglutarate, 25 μM $FeSO_4$, 0.5 mM dithiothreitol (DTT), 0.1 mM ascorbate, and either 2 mM D,L-End, 1 mM L-Arg, or 1 mM dideoxy-MPP-γ. Reaction mixtures were incubated at 30ºC for various times, the protein was precipitated, and the supernatant was treated with dansyl chloride (DNS-Cl) to permit HPLC analysis with UV detection (the assay containing dideoxy-MPP-γ did not require derivatization) [4]. When D,L-End was used as a substrate, a new peak appeared in the HPLC chromatogram that was dependent on MppO, Fe(II), and α-ketoglutarate (Figure 4B). The product was confirmed to be βhEnd by coinjection analysis with authentic βhEnd obtained from the acid hydrolysate of MPP. There were no detectable products when L-Arg or dideoxy-MPP-γ were used as substrate.

Because the enduracididine used as substrate in the MppO assays was obtained by hydrolysis of dideoxy-MPP, both D and L forms were present. To examine the stereospecificity of MppO, samples of D,L-End were preincubated with either D-amino acid oxidase (D-AAO) or L-amino acid oxidase (L-AAO) to destroy the D and L isomers, respectively. Preincubation of D,L-End with L-AAO resulted in a significant decrease in the amount of βhEnd produced by MppO (Figure 4C). The small amount of βhEnd still detected is presumably due to incomplete removal of L-End. Preincubation with D-AAO had no effect on product formation (Figure 4C). Hence, MppO specifically hydroxylates L-End and catalyzes the overall reaction illustrated in Figure 4D.

MppO, CS, and VioC all introduce a hydroxyl group at the β carbon of L-Arg or a derivative. Unlike CS and VioC, MppO oxidation does not facilitate subsequent cyclization involving the β carbon. Rather, the γ carbon of L-Arg must be activated for cyclization. Analogous to the biosynthesis of capreomycidine, the formation of End may involve γ-hydroxyarginine and a PLP-dependent γ-replacement reaction. Following *mppO* in the MPP cluster are candidate genes (*mppP* and *mppQ*) for the putative PLP-dependent enzyme, but a gene for a second hydroxylase has not been identified (N.A.M. et al., submitted). Characterization of MppP and MppQ is currently underway to determine their possible role in the formation of L-enduracididine.

Significance

Much of the diversity in nonribosomal peptides stems from the incorporation of unusual nonproteinogenic amino acids, including many of the common amino acids with β-hydroxyl groups. Hydroxylation can occur on carrier protein bound or free amino acids, and these hydroxyls are important for target recognition, peptide glycosylation, as sites of macrolactone cyclization, and as means to facilitate further alteration at the β carbon. To our knowledge, MppO is the first enzyme shown to catalyze the β-hydroxylation of a nonproteinogenic amino acid, and this study further expands our understanding of the formation of these key residues in numerous bioactive peptides.

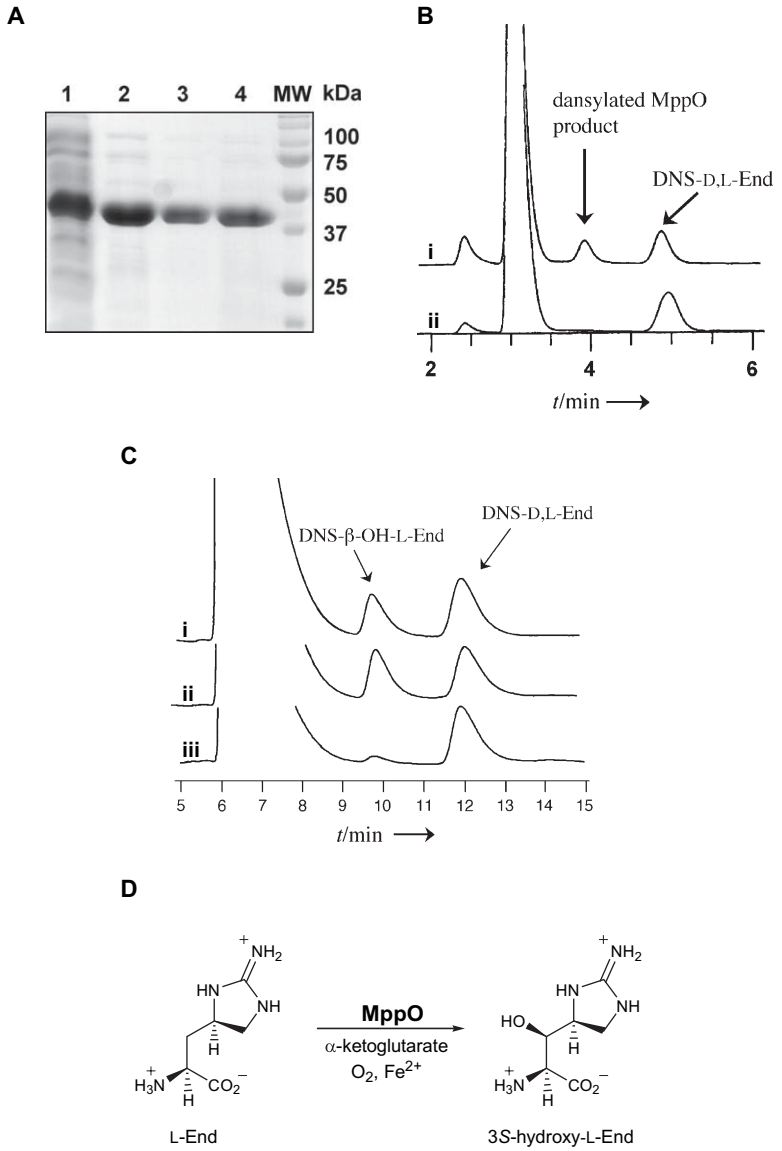

Figure 4. Heterologous Expression and Characterization of His_6-MppO

(A) SDS-PAGE analysis of the expression in *E. coli* and purification of His_6-MppO. Lane 1, soluble protein; lane 2, protein eluted from Co^{2+} affinity column in 150 mM buffered imidazole; lanes 3 and 4, protein eluted from Co^{2+} affinity column in 250 mM buffered imidazole. The calculated MW of His_6-MppO is 38.6 kDa.

(B) RP-HPLC analysis of the MppO assay: (i) complete MppO assay; (ii) assay with boiled MppO.

(C) RP-HPLC analysis of the substrate stereospecificity of MppO: (i) control MppO assay with untreated D,L-End; (ii) MppO assay in which the D,L-End was preincubated with D-amino acid oxidase for 1 hr; (iii) MppO assay in which the D,L-End was preincubated with L-amino acid oxidase for 1 hr.

(D) Proposed reaction catalyzed by MppO.

Experimental Procedures

Bacterial Strains, Cosmids, and Culture Conditions

Cosmid pNWA117 in the SuperCos1 vector contained the portion of the mannopeptimycin biosynthetic cluster containing *mppO* (N.A.M. et al., submitted). Unless otherwise described, *S. hygroscopicus* strains were cultured and preserved as previously described (N.A.M. et al., submitted). NovaBlue *E. coli* competent cells (Novagen) were used for all cloning. All *E. coli* strains were grown in liquid or on solid Luria-Bertani medium at 37ºC. Apramycin (50 μg/ml), kanamycin (50 μg/ml), chloramphenicol (25 μg/ml), nalidixic acid (25 μg/ml), and ampicillin (100 μg/ml) were used for selection of recombinant strains.

DNA Isolation, Manipulation, and Cloning

Standard protocols for DNA manipulation and Southern hybridization were followed [15]. Plasmid and cosmid DNA was isolated from *E. coli* strains by using Qiagen mini-prep kits (Qiagen). Isolation of DNA fragments from agarose was carried out with the Qiagen gel clean kit (Qiagen). Restriction and DNA-modifying enzymes were purchased from New England Biolabs. Genomic DNA was isolated from *S. hygroscopicus* strains as previously described (N.A.M. et al., submitted).

PCR was performed by using KOD Hot Start polymerase (Novagen) containing 5% (v/v) DMSO as recommended by the supplier. Primers were used at a final concentration of 0.5 μM, and the thermal cycling parameters were: one cycle of 96ºC × 4 min, 30 cycles of 96ºC × 1 min, annealing temperature (varied for each primer pair) × 1 min, 72ºC × 1.5 min, and one cycle of 72ºC × 10 min. PCR products were cloned by using the Zero Blunt TOPO Cloning Kit (Invitrogen).

Inactivation of *mppO* in *S. hygroscopicus* NRRL 30439

mppO was inactivated by insertional mutatagenesis with the kanamycin gene (*aphII*) from pFD666 [16]. Fragments of DNA flanking *mppO* were amplified by PCR. The upstream region was amplified by using primers *mppO*KOlft-for (5′-CTGAATTCGACCACGCCCGGATCATC-3′, EcoRI site underlined) and *mppO*KOlft-rev (5′-CTGGAGTTCGTCAGCCACACG-3′, half a PvuII site underlined) and an annealing temperature (T_a) of 72.2ºC. The downstream region was amplified by using primers *mppO*KOrt-for (5′-TTCAGCTGATCGACGACGCCATGTCC-3′, PvuII site underlined) and *mppO*KOrt-rev (5′-TATCTAGAGGTTGGCCCAGTGGAACG-3′, XbaI site underlined) and a T_a of 68.9ºC. *aphII* was amplified by using primers Kan-for (5′-AATTATCGAGGTTGACATC-3′) and Kan-rev (5′-TCAGAAGAACTCGTCAAG-3′) and a T_a of 58.2ºC. Primer Kan-for possessed a 5′ phosphate. The conjugatable suicide vector pBWV1 was constructed by digesting

pUC19 with SspI and inserting the *oriT* sequence amplified from pNWA200 (N.A.M. et al., submitted) by using primers *oriT*FOR (5′-TTGCCTTGCTCGTCGGTGA-3′) and *oriT*REV (5′-CGCACGATATACAGGATTTTGC-3′) and a T_a of 63.6ºC. To assemble the disruption construct, all four appropriately digested fragments were mixed and ligated by using T4 DNA ligase. *E. coli* transformants were plated on LB agar containing ampicillin and kanamycin.

The resulting construct (pBWA29) was introduced into *S. hygroscopicus* NRRL 30439 by conjugation from *E. coli* ET12567 carrying the nontransmissible plasmid pUZ8002 as previously described (N.A.M. et al., submitted). To identify exconjugants that had undergone a double crossover, genomic DNA from the wild-type and mutant colonies were cleaved with PmlI and MscI and were hybridized with a 1.2 kb *mppO*-containing PCR product amplified from genomic DNA of *S. hygroscopicus* NRRL 30439 by using the primers *mppO*compFOR (5′- AATCTAGAAGGAAGTAAAGGTTATGGAACG-3′) and *mppO*compREV (5′- TTTCTAGAGGCAGCCGGTCAGTAGATG-3′).

Analysis of Secondary Metabolite Production

S. hygroscopicus strains were fermented as described elsewhere (N.A.M. et al., submitted). Chromatographic analysis and purification of MPPs was performed as previously reported [2]. High-resolution FTMS analysis was performed by the Discovery Analytical Chemistry department at Wyeth Research. For the coinjection experiment, samples were dissolved in MeOH:H_2O to a final concentration of 1 mg/ml. An aliquot of the putative dideoxy-MPP-γ solution was combined with an equal volume of the solution containing authentic dideoxy-MPP-γ and -δ. Samples were analyzed on an Agilent 1100 system coupled with a Thermo-Finnigan LCQ Deca mass spectrometer equipped with an APESI source. The samples were chromatographed with 5%–50% B in A over 14 min with a flow rate of 0.3 ml/min on a YMC ODS-A column (2.0 × 100 mm) (A = H_2O/0.025% formic acid; B = MeCN/0.025% formic acid).

Sequence Analysis of the Chemically Mutagenized Dideoxy-MPP Producer

The *mppO* DNA sequence of the mutagenized and wild-type strains was amplified from the genomic DNA of each strain by PCR by using primers *mppO*compFOR and *mppO*compREV. PCR products were cloned by using the Zero Blunt TOPO Cloning Kit. Eight clones from each strain were picked for analysis, and their insert DNA completely sequenced on both strands. DNA sequences were compared by using the Sequencher sequence analysis program (Gene Codes Corp.).

Functional Expression and Characterization of MppO

To generate an *mppO* expression construct, primers Orf13f (5′-GGACATATGCTGACGCTCCACCTG-3′, NdeI site underlined), and Orf13r (5′-CAAGAATTCTCAGTAGATGAC-3′, EcoRI site underlined) were used to amplify *mppO* by PCR. The gel-purified amplicon was sequenced and then cloned into the NdeI and EcoRI sites of pET28a (Novagen) to yield plasmid pET28a/*mppO*. Expression was carried out by using *E. coli* Rosetta(DE3) cells (Novagen) as previously described [4], except that protein expression was induced with 1 mM isopropyl-β-D-thiogalactopyranoside. The culture was harvested, the cells were lysed, and a clarified cell-free extract was applied to a column of BD Talon Metal Affinity Resin (BD Biosciences) according to the manufacturer's directions. His_6-MppO was eluted in a step-wise fashion by using buffer containing 150 mM or 250 mM imidazole. Efficiency of purification was verified by SDS-PAGE. His_6-MppO fractions eluting in 250 mM imidazole were pooled and dialyzed against PBS to remove imidazole and were stored at either 4ºC or −80ºC.

Oxygenase assays were conducted as described previously by using appropriately diluted MppO in a total volume of 200 μl [4]. Substrates evaluated in this study included 2 mM D,L-End, 1 mM L-Arg, and 1 mM dideoxy-Mpp-γ. Reactions were initiated by the addition of MppO and were incubated at 30ºC for 2–6 hr.

To analyze the MppO reaction, substrates and products were derivatized by treatment with dansyl chloride and were analyzed by RP-HPLC as previously described [4]. Assays that included L-Arg or L-End as substrate were evaluated under isocratic conditions of 80% 50 mM NH_4OAc (pH 5.5) and 20% MeCN. These reactions were analyzed by using a 25 min linear gradient from 10% A to 50% B (A = 0.05% aqueous formic acid, B = MeCN with 0.05% formic acid).

To determine the stereospecificity of MppO, preincubation experiments were conducted in 40 mM Tris, 80 mM KCl (pH 8.5) and included 25 mM D,L-End and 0.2 U porcine kidney D-AAO or 0.8 U L-AAO from *Crotalus adamanteus* venom in a total volume of 40 μl. Reactions were initiated with substrate and were incubated at 37ºC for 1 hr. The reaction mixtures were centrifuged at 18,000 × g for 1 min, and 20 μl aliquots were removed and used as substrate in MppO assays conducted as described above.

Acknowledgments

This work was supported in part by the National Institutes of Health (grant GM69320 to T.M.Z.). We thank Quan Zhang for technical assistance, Dr. Edmund Graziani for providing D,L-End samples, Dr. Jason Lotvin for providing *S. hygroscopicus* strains NRRL 30450 and NRRL 30443, and Dr. Xidong Feng for conducting the high-resolution FTMS analysis.

Received: May 31, 2005
Revised: September 1, 2005
Accepted: September 21, 2005
Published: November 18, 2005

References

1. Singh, M.P., Petersen, P.J., Weiss, W.J., Janso, J.E., Luckman, S.W., Lenoy, E.B., Bradford, P.A., Testa, R.T., and Greenstein, M. (2003). Mannopeptimycins, new cyclic glycopeptide antibiotics produced by *Streptomyces hygroscopicus* LL-AC98: antibacterial and mechanistic activities. Antimicrob. Agents Chemother. *47*, 62–69.
2. He, H., Williamson, R.T., Shen, B., Graziani, E.I., Yang, H.Y., Sakya, S.M., Petersen, P.J., and Carter, G.T. (2002). Mannopeptimycins, novel antibacterial glycopeptides from *Streptomyces hygroscopicus*, LL-AC98. J. Am. Chem. Soc. *124*, 9729–9736.
3. Jackson, M.D., Gould, S.J., and Zabriskie, T.M. (2002). Studies on the formation and incorporation of streptolidine in the biosynthesis of the peptidyl nucleoside antibiotic streptothricin F. J. Org. Chem. *67*, 2934–2941.
4. Yin, X., and Zabriskie, T.M. (2004). VioC is a non-heme iron, α-ketoglutarate dependent oxygenase that catalyzes the formation of 3*S*-hydroxy-L-arginine during viomycin biosynthesis. ChemBioChem *5*, 1274–1277.
5. Ju, J., Ozanick, S.G., Shen, B., and Thomas, M.G. (2004). Conversion of (2*S*)-arginine to (2*S*,3*R*)-capreomycidine by VioC and VioD from the viomycin biosynthetic pathway of *Streptomyces* sp. strain ATCC11861. ChemBioChem *5*, 1281–1285.
6. Yin, X., McPhail, K.L., Kim, K.-J., and Zabriskie, T.M. (2004). Formation of the nonproteinogenic amino acid 2*S*,3*R*-capreomycidine by *vioD* from the viomycin biosynthesis pathway. ChemBioChem *5*, 1278–1281.
7. Yin, X., O'Hare, T., Gould, S.J., and Zabriskie, T.M. (2003). Identification and cloning of genes encoding viomycin biosynthesis from *Streptomyces vinaceus* and evidence for involvement of a rare oxygenase. Gene *312*, 215–224.
8. Thomas, M.J., Chan, Y.A., and Ozanick, S.J. (2003). Deciphering tuberactinomycin biosynthesis: isolation, sequencing and annotation of the viomycin biosynthetic gene cluster. Antimicrob. Agents Chemother. *47*, 2823–2830.
9. Busby, R.W., Chang, M.D.-T., Busby, R.C., Wimp, J., and Townsend, C.A. (1995). Expression and purification of two isozymes of clavaminate synthase and initial characterization of the iron binding site. J. Biol. Chem. *270*, 4262–4269.
10. Que, L., and Ho, R.Y.N. (1996). Dioxygen activation by enzymes with mononuclear non-heme iron active sites. Chem. Rev. *96*, 2607–2624.
11. Khaleeli, N., Busby, R.W., and Townsend, C.A. (2000). Site-directed mutagenesis and biochemical analysis of the endogenous ligands in the ferrous active site of clavaminate synthase. The His-3 variant of the 2-His-1-carboxylate model. Biochemistry *39*, 8666–8673.

12. Zhang, Z., Ren, J., Stammers, D.K., Baldwin, J.E., Harlos, K., and Schofield, C.J. (2000). Structural origins of the selectivity of the trifunctional oxygenase clavaminic acid synthase. Nat. Struct. Biol. *7*, 127–133.
13. Clifton, I.J., Doan, L.X., Sleeman, M.C., Topf, M., Suzuki, H., Wilmouth, R.C., and Schofield, C.J. (2003). Crystal structure of carbapenem synthase (CarC). J. Biol. Chem. *278*, 20843–20850.
14. Elkins, J.M., Ryle, M.J., Clifton, I.J., Dunning Hotopp, J.C., Lloyd, J.S., Burzlaff, N.I., Baldwin, J.E., Hausinger, R.P., and Roach, P.L. (2002). X-ray crystal structure of *Escherichia coli* taurine/α-ketoglutarate dioxygenase complexed to ferrous iron and substrates. Biochemistry *41*, 5185–5192.
15. Sambrook, J., and Russell, D.W. (2001). Molecular Cloning: A Laboratory Manual, Third Edition (New York: Cold Spring Harbor Laboratory Press).
16. Denis, F., and Brzezinski, R. (1992). A versatile shuttle cosmid vector for use in *Escherichia coli* and actinomycetes. Gene *111*, 115–118.
17. Hojati, Z., Milne, C., Harvey, B., Gordon, L., Borg, M., Flett, F., Wilkinson, B., Sidebottom, P.J., Rudd, B.A.M., Hayes, M.A., et al. (2002). Structure, biosynthetic origin, and engineered biosynthesis of calcium-dependent antibiotics from *Streptomyces coelicolor*. Chem. Biol. *9*, 1175–1187.